An overview of the LIDAR observations of asteroid 25143 Itokawa

Mukai, Tadashi ; Abe, Shinsuke ; Hirata, N. ; Nakamura, R. ; Barnouin-Jha, O. S. ; Cheng, A. F. ; Mizuno, T. ; Hiraoka, K. ; Honda, T. ;…

(Citation)
Advances in Space Research,40(2):187-192

(Issue Date)
2007

(Resource Type)
journal article

(Version)
Accepted Manuscript

Elsevier Editorial System(tm) for JASR 2006

Manuscript Draft

Manuscript Number:

Title: An Overview of the LIDAR Observations of Asteroid 25143 Itokawa

Article Type: Contributed Paper

Section/Category: B0.4 - Small Bodies Exploration

Keywords: asteroids; Itokawa; LIDAR; mass; density

Corresponding Author: Dr. Tadashi Mukai,

Corresponding Author's Institution: Graduate School of Science and Technology

First Author: Tadashi Mukai

Order of Authors: Tadashi Mukai; S. Abe ; N. Hirata ; R. Nakamura; O. S Barnouin-Jha ; A, F Cheng; T. Mizuno ; K, Hiraoka ; T. Honda ; H. Demura ; R. W Gaskell; T. Hashimoto ; T. Kubota ; M. Matsuoka; D. J Scheeres; M. Yoshikawa

Abstract: We present an overview of laser altimeter's results of asteroid 25143 Itokawa. A trace of beam spot with elliptic shape of 7m x 12m made the local surface topography possible in the accuracy of a few meter in altitude from home position at an altitude of roughly 7 km from the surface. A sequential detection of altitude of spacecraft during the descent phase for sampling provided the mass of asteroid of (3.58+-0.18) x 10^10 kg. Combined with total volume of asteroid deduced by shape model, i.e. (1.84+-0.09) x 10^7 m^3, it is found that the asteroid Itokawa has low density of (1.95+-0.14) g/cm^3, and consequently a high bulk porosity of about 40%.

An Overview of the LIDAR Observations of Asteroid 25143 Itokawa

T. Mukai [(1)], S. Abe [(1)], N. Hirata [(5)], R. Nakamura [(2)], O. S. Barnouin-Jha [(3)], A. F. Cheng [(3)], T. Mizuno [(4)], K. Hiraoka [(1)], T. Honda [(1)], H. Demura [(5)], R. W. Gaskell [(6)], T. Hashimoto [(4)], T. Kubota [(4)], M. Matsuoka [(7)], D. J. Scheeres [(8)], and M. Yoshikawa [(4)]

[(1)] Graduate School of Science and Technology, Kobe University, Nada, Kobe 657-8501, Japan,
[(2)] National Institute of Advanced Industrial Science and Technology, Tsukuba 305-8568, Japan,
[(3)] The Johns Hopkins University, Applied Physics Laboratory, Laurel, MD 20723-6099, USA,
[(4)] Institute of Space and Astronautical Science, Japan Aerospace Exploration Agency, Sagamihara, Kanagawa 229-8510, Japan,
[(5)] Department of Computer Software, University of Aizu, Aizuwakamatsu, Fukushima 965-8580, Japan,
[(6)] Jet Propulsion Laboratory, California Institute of Technology, Pasadena, CA 91109, USA,
[(7)] NEC Aerospace Systems, Yokohama, Kanagawa 224-0053, Japan,
[(8)] Department of Aerospace Engineering, University of Michigan, Ann Arbor, MI 48109-2140, USA.

Abstract

We present an overview of laser altimeter's results of asteroid 25143 Itokawa. A trace of beam spot with elliptic shape of 7m×12m made the local surface topography possible in the accuracy of a few meter in altitude from home position at an altitude of roughly 7 km from the surface. A sequential detection of altitude of spacecraft during the descent phase for sampling provided the mass of asteroid of $(3.58\pm0.18)\times10^{10}$ kg. Combined with total volume of asteroid deduced by shape

model, i.e. $(1.84\pm0.09)\times10^7$ m^3, it is found that the asteroid Itokawa has low density of (1.95 ± 0.14) g/cm^3, and consequently a high bulk porosity of about 40%.

1. Introduction

The spacecraft for asteroid sample return, HAYABUSA (falcon in Japanese), arrived at near-Earth S-type asteroid, 25143 Itokawa in September 2005, and in-situ measurements were successfully performed during a stay near Itokawa by the end of November 2005.

Major science objectives of HAYABUSA were to obtain the following information for surface materials and structure of target asteroid, and derive the origin and current nature of the asteroid. That is, (1) global chemical and mineralogical information by orbiter remote sensing instruments, (2) local microscopic information by micro-rover instrument landed on the surface of target asteroid, (3) determination of bulk density of asteroid by laser altimeter (LIDAR) and visible camera (AMICA) together with the range and Doppler from ground stations, and (4) determination of mineralogical, chemical, isotropic abundance of surface material from collected samples.

The objectives (1) and (3) were successfully performed, and a part of their results has been already published elsewhere (e.g., Fujiwara et al. 2006, Abe et al. 2006). However, unfortunately, micro-rover failed to land on the surface, and consequently objective (2) was cancelled. Furthermore, the collection of samples from the surface has not yet been confirmed (see, e.g. Yano et al. 2006). We will learn the result of sample collection when the capsule for sample materials will come back to Earth in June 2010.

In this paper, we will focus on the scientific results obtained by one of orbiter remote sensing instruments, i.e. a laser altimeter (LIDAR), related to the subject (3) and the topics of surface albedo and local topography.

2. LIDAR scientific results

Original science objectives of LIDAR (Mukai et al. 2002) were planned to detect (1)

surface structure and shape of asteroid via systematic survey from home position (altitude of roughly 7 km from the surface) associated with in situ measurements by visible imaging camera (AMICA) and near-infrared spectroscopic instrument (NIRS), and (2) mass of asteroid via free-fall of spacecraft.

2.1. Surface topography

In pulse generator of the LIDAR, a timing clock starts at the time of the pulse ejection to the target, and stops when the receiver gets a signal of the reflected pulse from the target. Since the frequency of the timing clock is 75 MHz, the accuracy of the ranging at a distance of 50m from the target becomes 1m. On the other hand, the accuracy at a 50km-distance as 10m was estimated from the expected S/N ratio when the asteroid has a Lambert scattering surface with an albedo of 0.05. The first signal of reflected laser light was recorded on 10 September, 2005 when the spacecraft was at about 49 km from the asteroid.

As shown in Fig.1, total of 4,107,104 shots were generated by LIDAR during the phase of in situ measurements (about 3 months), and 1,665,548 returned signals were successively detected by LIDAR. It had been tested in pre-flight experiments that the pulse generator can keep its constant intensity at least by 1.5×10^8 shots. No significant decline of intensity of laser beam occurred during the mission near the asteroid Itokawa. Failures in two of three reaction wheels on the spacecraft HAYABUSA on 2 October dramatically reduced the hit rate, i.e. a ratio of numbers of returned shots to total shots (see Fig.1).

The resulting fluctuation of beam spot on the surface due to loss of reaction wheels made systematic surface survey difficult (see Fig.2). Although the systematic survey could not be performed, LIDAR cloud of data almost covered the whole surface of asteroid, except both polar regions. These data make possible to study the local topography, where a typical size of beam spot on the surface is 7m×12m with an elliptic shape and accuracy of altitude is about a few meters in the measurements at the home position (see Fig.2). Blocks with about 3- to 4-m elevation and horizontal size of the order of the LIDAR spot are detected as shown in Fig.2. Abe et al. (2006) also indicatedthe existence of such blocks on the surface

2.2. Albedo measurement

In the original plan for LIDAR science objective, the measurement of surface albedo was not included explicitly. The detection of surface albedo was optional plan, because LIDAR instrument has no function to detect the intensities of generated laser light and received reflected light simultaneously. As shown in Fig.3, the variation of intensity of received reflected light was recorded during the descending phase of spacecraft. An automatic change of dynamic range of sensitivity of detector can be analyzed by the data of instrument status, and consequently we can derive the variation of intensity of reflected light, when the received intensity is normalized by the altitude of spacecraft. When the intensity of generated laser light kept constant during the detection, the data of normalized reflected light intensity provide the information of surface albedo. Since our LIDAR instrument could change the mode to monitor the intensity of generated laser light by telemetry, we sent the command at some intervals to measure the intensity of generated laser light during the mission period of LIDAR detection.

The pulse generator consists of the Nd:YAG laser with a wavelength of 1064nm and Q-switch pumped by the laser diode (LD). The wavelength pumped by the LD is sensitive to the temperature, and consequently the intensity of the generated pulse by the LIDAR strongly depends on the temperature. To keep a constant strength of the LIDAR pulse, the thermostat and the panel for heater emission are set for the LIDAR instrument. In Fig. 4, the time variations of temperature of LD and intensity of generated pulse monitored in situ are presented. It is found that both vary randomly with time, and as a result we have to be prepared a relatively large uncertainty of intensity of generated pulse. It will need further study of intensity variation of generated pulse to estimate the surface albedo from the LIDAR data.

From the ground-based observations, Cellino et al.(2005) reported a value of albedo in V band, 0.24±0.01 based on the polarimetric observations, and Mueller et al. (2005) presented a value of albedo, 0.19(+0.11, -0.03) based on the infrared observations. Both values of albedo are consistent with that estimated for the S-type taxonomic classification of asteroid Itokawa.

Saito et al. (2006) reported based on AMICA data that on the surface of Itokawa, the brighter region is bluer in visible color, while the darker is redder in visible color. A more than 10% variation of the albedo appears between rough terrain and smooth area.

Although a relative variation of the reflected light intensity is derived over the whole surface of Itokawa by AMICA, the absolute value of albedo has not yet been reported due to late processing of calibration data of sensitivity at the wavelengths of AMICA bands.

2.3. Mass estimation

It is important to apply a reasonable shape model of asteroid Itokawa to know the relative position of spacecraft to the surface of Itokawa. In addition, the center of mass of asteroid plays an important role to derive the gravitational force on the spacecraft. As shown in Abe et al. (2006), we have used the shape model of Itokawa derived by AMICA data by Demura et al. (2006), where the volume of asteroid is $(1.84\pm0.09)\times10^{7}$ m^3. Our value of mass of Itokawa becomes $(3.58\pm0.18)\times10^{10}$ kg and, consequently the density of Itokawa is estimated as (1.95 ± 0.14) g/cm^3.

It should be noted that our error in mass estimation is significantly larger than that by the NLR in NEAR mission, i.e. the error was 0.0001% expected in mass by the NLR, and a resulting value of mass of asteroid Eros has a small error in mass as $(6.687\pm0.003)\times10^{15}$ kg (Yeomans et al. 2000). A large error in our mass estimation comes from the fact that the HAYABUSA did not take an orbit rounding the asteroid, and an available time to measure the gravity force by LIDAR was very short. Namely, the reported value of mass in Abe et al. (2006) has been estimated from the data obtained for about 45 min on 11 November, 2005 during the descending phase of spacecraft for sampling from the altitude of 1227 to 825 m. Moreover, since thrusting force at the altitude of 1km was about 30% of that of gravity force of Itokawa, which is 6 times larger than radiation pressure, most of mass' error caused by estimation error of thrusting force.

When assuming a LL meteorite composition (density of 3.19 g/cm^3), the resulting density of Itokawa suggests a high bulk porosity of about 40%. The porosity of 40% is similar to those reported in 253 Mathilde, 90 Antipole, and 48 Eugenia (Britt et al.

2002). These three asteroids are classified as C-type and their masses are larger more than seven orders of magnitude, compared with the mass of Itokawa. The internal structure of high porous asteroid is assumed as loosely consolidated (rubble pile) structures (see Britt et al. 2002). Therefore, we can conclude that asteroid Itokawa is the first recognized small S-type asteroid with rubble pile structure.

3. Conclusions

We briefly summarized the LIDAR results concerning the mass and surface properties of small (535×294×209m) S-type asteroid Itokawa. Combined the volume derived by the shape model from AMICA data, our mass value of $(3.58\pm0.18)\times10^{10}$ kg suggests low mass density of Itokawa, (1.95 ± 0.14) g/cm^3, and high bulk porosity of 40%. Concerning the local surface topography, our data of LIDAR revealed the existence of boulders with a few meters in size on the surface of Itokawa. Full analysis of LIDAR data will be completed near future, and present the surface map of roughness with the accuracy of several meters in altitude, as well as albedo map.

Acknowledgement

This research was supported by "The 21st Century COE Program of Origin and Evolution of Planetary System" in the Ministry of Education, Culture, Sports, Science, and Technology.

References

Abe, S., Mukai, T., Hirata, N., et al., Mass and local topography measurements of Itokawa by Hayabusa, Science 312, 1344-1347, 2006.

Britt, D.T., Yeomans, D., Housen, K. and Consolmagno, G. Asteroid density, porosity,

and structure, Asteroids III (eds. Bottke Jr. W.F. et al.) Arizona Press, 485-515, 2002.

Cellino, A., Yoshida, F., Anderlucci, E., et al., A polarimetric study of asteroid 25143 Itokawa, Icarus 179, 297-303, 2005.

Demura, H., Kobayashi, S., Nemoto, E., et al., Pole and Global Shape of 25143 Itokawa, Science 312, 1347-1349, 2006.

Fujiwara, A., Kawaguchi, J., Yeomans, D. K., et al., The rubble-pile asteroid Itokawa as observed by Hayabusa, Science 312, 1330-1334, 2006.

Mueller, T.G., Sekiduchi, T., Kaasalainen, M., et al., Thermal infrared observations of the Hayabusa spacecraft target asteroid 25143 Itokawa, A&A 443, 347-355, 2005.

Mukai, T., Araki, H., Mizuno, T., et al. Detection of mass, shape and surface roughness of target asteroid of MUSES-C by LIDAR, Adv. Space Research 29, 1231-1235, 2002.

Saito, J., Miyamoto, H. Nakamura, R., et al., Detailed Images of Asteroid 25143 Itokawa from Hayabusa, Science 312, 1341-1344, 2006.

Yano, H., Kubota, T., Miyamoto, H., et al., Touchdown of the Hayabusa spacecraft at the Muses-Sea on Itokawa, Science 312, 1350-1353, 2006.

Yeomans, D. K., Antreasian, P. G., Barriot, J.-P., et al., Radio science results during the NEAR-Shoemaker spacecraft rendezvous with Eros, Science 289, 2085-2088, 2000.

Figure captions

Fig.1. LIDAR fit rate during the mission of HAYABUSA near asteroid Itokawa from September 10 to November 25, 2005. Failures in two of the three reaction wheels occurred on October 2, 2005.

Fig.2a. Fluctuation of LIDAR spot on the surface of asteroid Itokawa.

Fig.2b. An area detected by LIDAR in Fig.2a, noted as square on the smooth area called Muses-C.

Fig.3. Time variations of altitude (in unit of m in the left vertical axis) and intensity of received laser light (in arbitrary unit between 0 and 250 in the right vertical axis).

Fig.4. Time variations of temperature of LIDAR instrument (solid line, in unit of ^{o}C in the left vertical axis) and intensity of generated pulse (dashed line, in arbitrary unit in the right vertical axis).

Figure

Fig.1. LIDAR fit rate during the mission of HAYABUSA near asteroid Itokawa from September 10 to November 25, 2005. Failures in two of the three reaction wheels occurred on October 2, 2005.

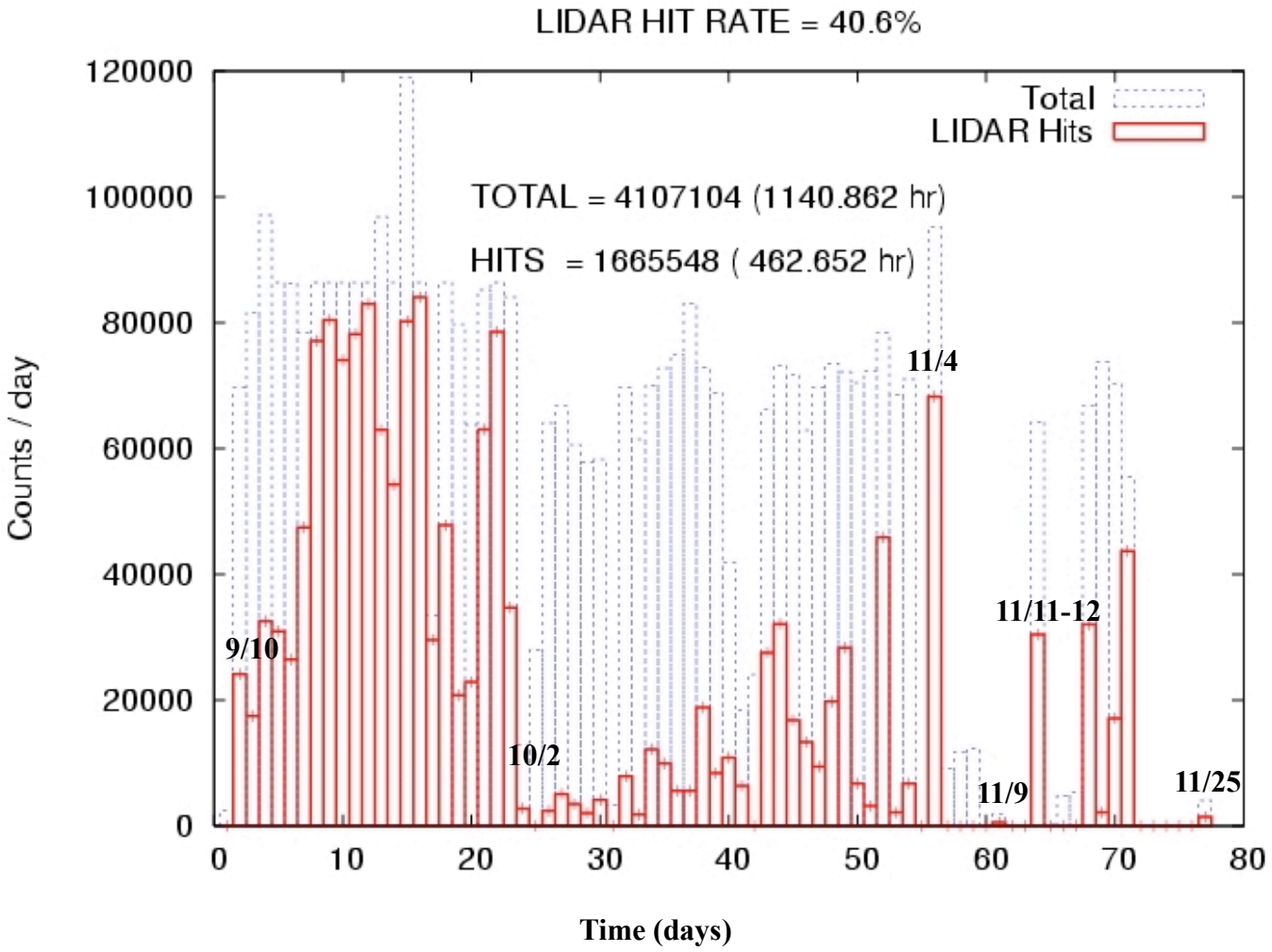

Fig.2a. Fluctuation of LIDAR spot on the surface of asteroid Itokawa.

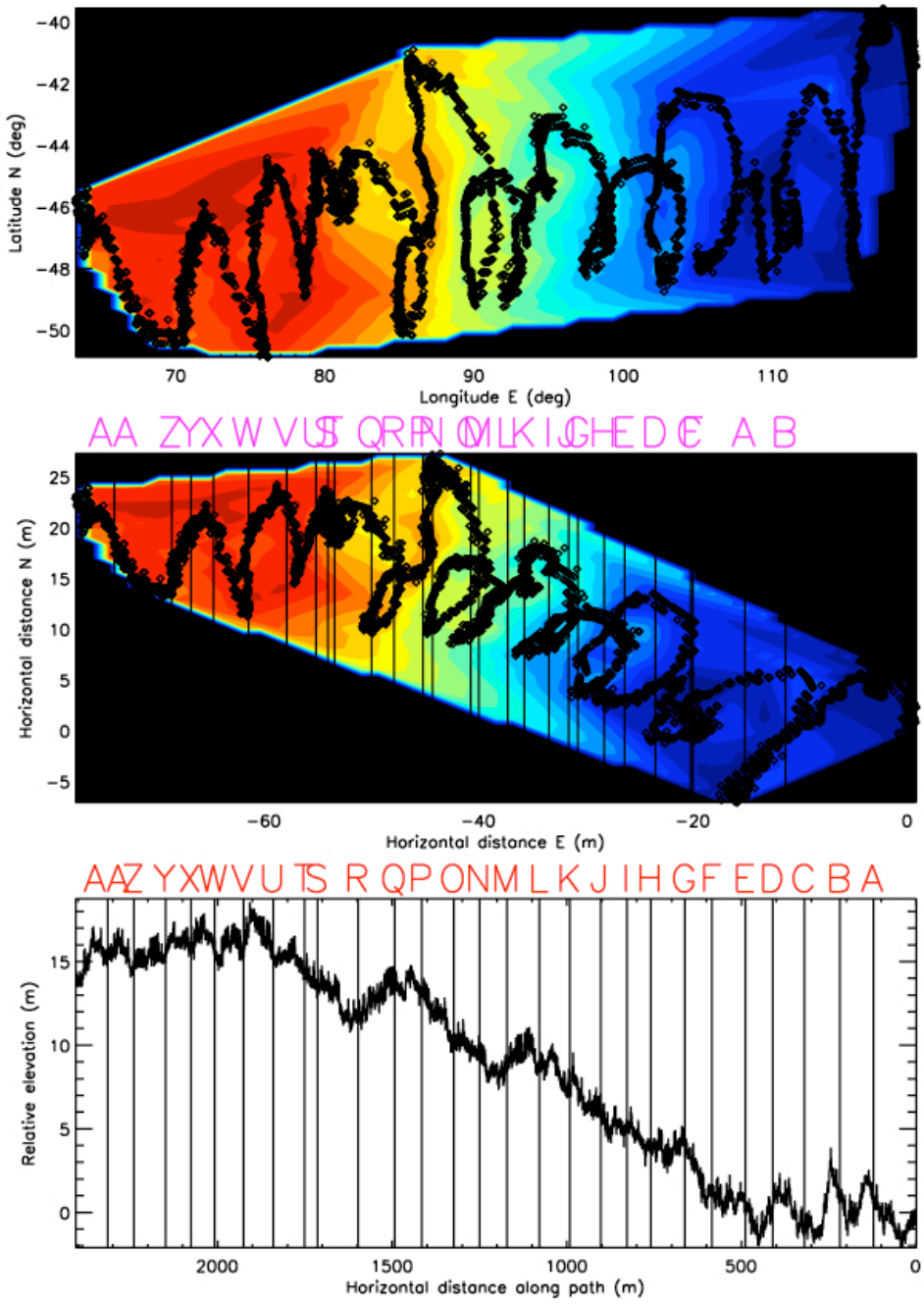

Fig.2b. An area detected by LIDAR in Fig.2a, noted as square on the smooth area called Muses-C.

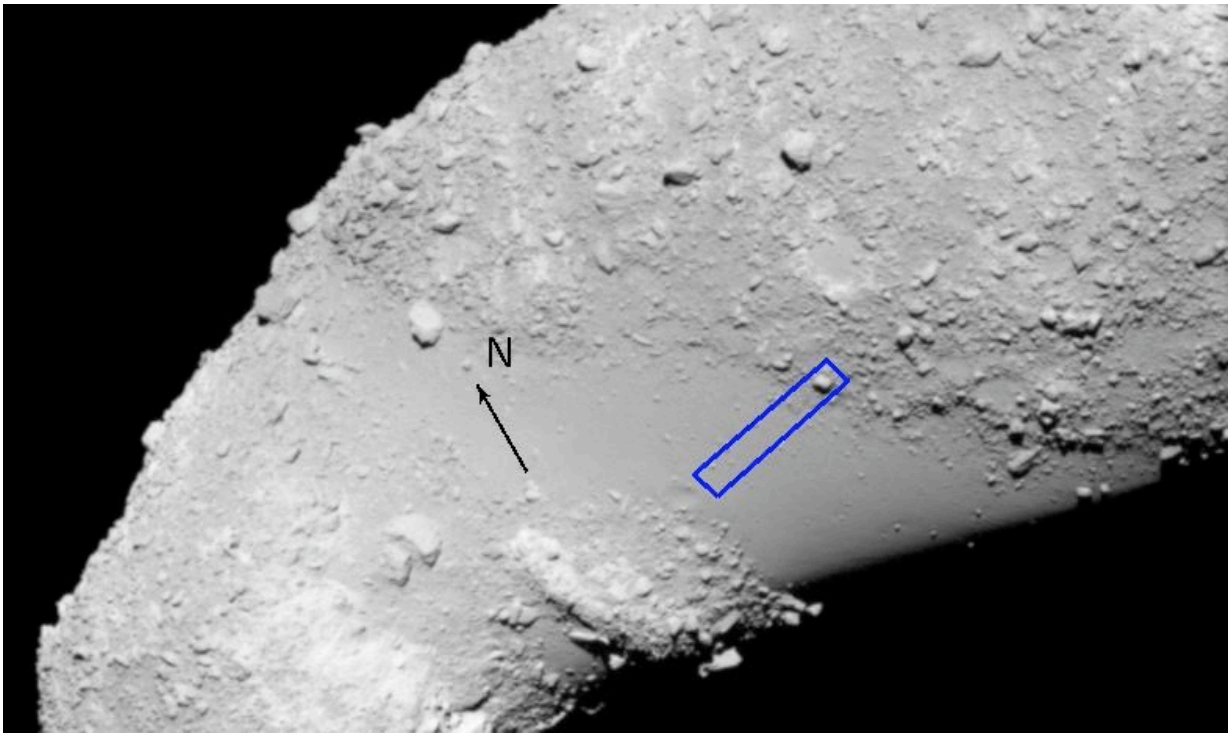

Fig.3. Time variations of altitude (in unit of m in the left vertical axis) and intensity of receiving laser light (in arbitrary unit between 0 and 250 in the right vertical axis).

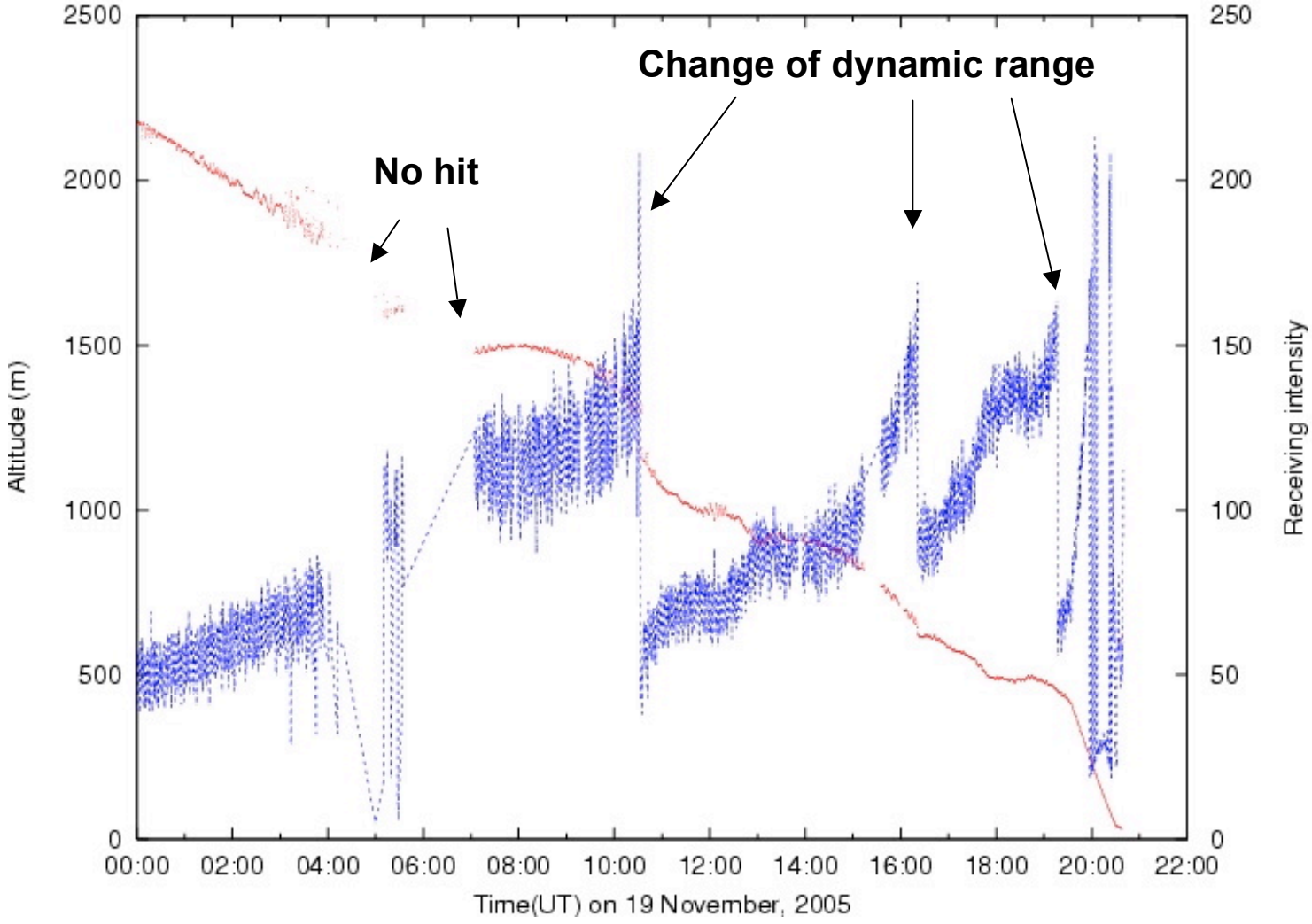

Fig.4. Time variations of temperature of LIDAR instrument (solid line, in unit of ^{o}C in the left vertical axis) and intensity of generated pulse (dashed line, in arbitrary unit in the right vertical axis).